6-1-1999

Piezoelectric and pyroelectric properties of ferroelectric Langmuir-Blodgett polymer films

A.V. Bune
University of Nebraska - Lincoln

Chuanxing Zhu
University of Nebraska - Lincoln

Stephen Ducharme
University of Nebraska - Lincoln, sducharme1@unl.edu

L.M. Blinov
Institute of Crystallography of the Russian Academy of Sciences, Moscow, Russia

V.M. Fridkin
Institute of Crystallography of the Russian Academy of Sciences, Moscow, Russia

See next page for additional authors

Piezoelectric and pyroelectric properties of ferroelectric Langmuir–Blodgett polymer films

A. V. Bune,[a] Chuanxing Zhu, and Stephen Ducharme[b]
Department of Physics and Astronomy and Center for Material Research and Analysis, University of Nebraska, Lincoln, Nebraska 68588-0111

L. M. Blinov, V. M. Fridkin, S. P. Palto, N. G. Petukhova, and S. G. Yudin
Institute of Crystallography of the Russian Academy of Sciences, 117333 Moscow, Russia

(Received 26 October 1998; accepted for publication 22 February 1999)

The piezoelectric and pyroelectric responses of ferroelectric Langmuir–Blodgett polymer films are less than the largest values measured with bulk films of the same composition. The films of the crystalline copolymer poly(vinylidene fluoride trifluoroethylene) fabricated by the Langmuir–Blodgett technique are 30 ML thick (15 nm) and are highly crystalline and oriented with polarization perpendicular to the film. Both piezoelectric and pyroelectric measurements show reversible ferroelectric switching. The films are suitable for use in pyroelectric infrared imaging and in piezoelectric acoustic transducers. © *1999 American Institute of Physics.* [S0021-8979(99)03311-3]

I. INTRODUCTION

Piezoelectric and pyroelectric effects are very well established in crystalline polyvinylidene fluoride (PVDF) and copolymer of vinylidene fluoride and trifluoroethylene P(VDF/TrFE) since the pioneering work of Kawai in 1969 (Ref. 1) and Bergman, McFee, and Crane in 1971.[2] But, there is still uncertainty about the mechanism and the contribution of the amorphous phase to piezoelectric and pyroelectric response.[3–5] Previous PVDF and copolymer P(VDF/TrFE) films are mixtures of crystalline and amorphous phases. Recently, our group has prepared ultrathin crystal copolymer P(VDF/TrFE) films by the Langmuir–Blodgett (LB) deposition technique, and demonstrated ferroelectricity in films as thin as 1 nm.[6–9] The goal of this work is the measurement of piezoelectric and pyroelectric responses in these high-quality ferroelectric copolymer P(VDF/TrFE) films.

II. EXPERIMENT

For the present study, ultrathin crystalline films of the random copolymer P(VDF/TrFE), containing 70% vinylidene fluoride and 30% trifluoroethylene were prepared by Langmuir–Blodgett deposition on a glass substrate covered by aluminum. The films are 30 ML (15 nm) thick and the electrode area was in the range 1–9 mm^2. An aluminum top electrode was evaporated to form a sandwich structure ready for electrical measurements. The polarization of the films was saturated in the direction perpendicular to the film plane at a dc voltage of 16 V (1.2 GV/m), well above the coercive field at approximately 12 V,[6] for at least 10 min. Film preparation is described in more detail elsewhere.[7] The high crystallinity and highly ordered structure of the films with carbon backbone chains aligned in the plane of the substrate was previously established by scanning tunneling microscopy measurements[7,8,10] and x-ray diffraction.[10]

A. Piezoelectric measurements

A high-resolution Mach–Zehnder interferometer[11] was adopted to measure sample strain for the piezoelectric measurements. The strain was caused by an external electric field through the inverse piezoelectric effect with piezoelectric coefficient d_{33} defined by

$$d_{33}^{T}=\left(\frac{\partial S_3}{\partial E_3}\right)_T, \tag{1}$$

where S is the strain induced by the applied electric-field E, and the stress T is constant. The x_3 axis is the direction of spontaneous polarization, which is perpendicular to the film surface. [We use contracted notation where the three-dimensional tensor d_{ijk} is represented by a two-dimensional d_{il}, where $l=1-6$ represents the six distinct combinations of the (j,k) indices.[12]] We must keep in mind that the film is clamped on a rigid substrate, and can expand or contract only in the direction perpendicular to the surface. So, the conditions are not truly stress free. Therefore, the measured piezoelectric response represents an effective coefficient.[13] Following Ref. 13, and taking into account the symmetry of the P(VDF/TrFE) films,[14] we measured the effective piezoelectric coefficient $d_{33}(\mathrm{eff})$:

$$\frac{S_3}{E_3}=d_{33}(\mathrm{eff})$$

$$=d_{33}^{T}+\frac{d_{32}^{T}(s_{12}s_{13}-s_{11}s_{23})+d_{31}^{T}(s_{12}s_{23}-s_{22}s_{13})}{s_{11}s_{22}-s_{12}^{2}}, \tag{2}$$

[a]Also at the Institute of Crystallography of the Russian Academy of Sciences, 117333, Moscow, Russia.
[b]Electronic mail: ducharme@unlinfo.unl.edu

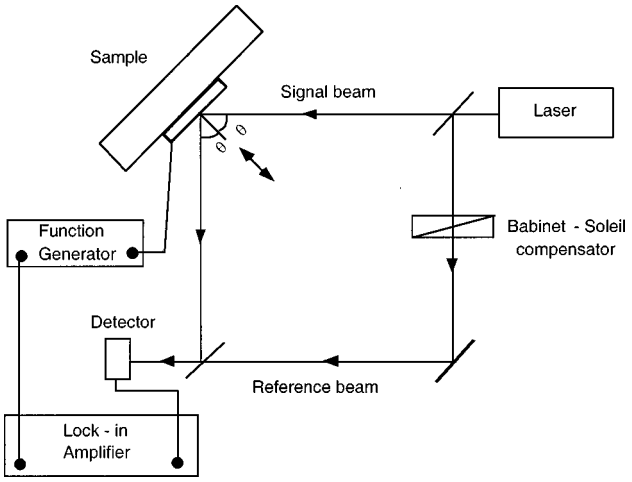

FIG. 1. Mach–Zehnder interferometer for measurement of piezoelectric strain.

where s_{ij} are the elastic compliance coefficients of the film and d_{3i}^T are the piezoelectric coefficients. In our experiments we use a modified Mach–Zehnder interferometer combined with an ac lock-in technique, as shown in Fig. 1, with a resolution of 10^{-3} nm or better. A He–Ne laser beam with wavelength 632 nm was focused to a 0.5 mm diameter on the sample. The bottom of the sample was glued to the sample holder placed at one corner of the signal arm, while the top of the sample was free to move so that any changes in the thickness of the sample induced by the piezoelectric effect caused a shift $\Delta\phi$ in the optical phase difference ϕ_o between the signal beam and reference beam. A Babinet–Soleil compensator was used as a variable thickness plate to adjust the phase difference to the most sensitive point ($\phi_o = \pm \pi/2$). A function generator provided both dc and ac voltage applied to the sample. The dc voltage served as a polarization field, while the small sinusoidal ac voltage at frequency $f = 1$ kHz acted as the piezoelectric driving field. The interferometer output at the driving frequency f was proportional to the piezoelectric coefficient. The induced phase change is

$$\Delta\phi = \frac{4\pi}{\lambda} \cos\theta d_{33}(\text{eff}) V_{\text{ac}}, \tag{3}$$

where λ is the wavelength of the light, and $\theta = 45°$ is the incidence angle of the beam into the sample surface and the refractive index of air is taken as 1. This phase change causes an intensity change in the interferometer:

$$\Delta I = \mp 2\sqrt{I_1 I_2}\, \sin(\Delta\phi) \approx \mp 2\sqrt{I_1 I_2}\Delta\phi, \tag{4}$$

when $\Delta\phi \ll 1$ and $\phi_o = \pm \pi/2$, where I_1 and I_2 are the intensity of the signal beam and reference beam, respectively, as measured individually at the detector. The intensity modulation ΔI was measured by the detector in combination with a lock-in amplifier referenced to the voltage modulation frequency f. The whole apparatus was mounted on a honeycomb optical table with air suspension and sealed into a black box to reduce mechanical and acoustical disturbances.

B. Pyroelectric measurements

Pyroelectric measurements were conducted by using both rapid laser modulation heating (Chynoweth method)[6,15] and slow heating/cooling methods.[16] For the Chynoweth modulation method, the sample was heated by the He–Ne laser 5 mW beam chopped at frequency $f = 1$ kHz. The pyroelectric current was measured by a lock-in amplifier (with 30 ms time constant) referenced to the chopper frequency f. The absolute value of the pyroelectric coefficient was measured by the slow heating/cooling method in a temperature-stabilized chamber. The pyroelectric current was measured as the sample was alternately heated and cooled at a constant rate ranging from 0.5 to 4 °C/min. The film can expand and contract only perpendicular to the surface, because the thermal expansion coefficient of the substrate is at least one order of magnitude less than the thermal expansion coefficient of the polymer, so the measured pyroelectric coefficient $p_3(\text{eff})$ consists of two contributions, the primary effect and the secondary effect:[12,17]

$$p_3(\text{eff}) = \left(\frac{\partial P_s}{\partial T}\right)_s + \frac{d_{33}^T \alpha_3^s}{s_{33}^s} = \left(\frac{I}{A}\right)\left(\frac{\partial T}{\partial t}\right)^{-1}, \tag{5}$$

where P_s is the spontaneous polarization, T is temperature, S is the strain, d_{33}^T is the stress-free piezoelectric coefficient, s_{33}^s is the elastic compliance coefficient, α_3^s is the thermal expansion coefficient, I is the pyroelectric current, A is the surface area, and $\partial T/\partial t$ is the rate of temperature change. The pyroelectric current was measured by a Keithly 428 current amplifier. The temperature of the film was measured by a copper–constantan thermocouple with an absolute accuracy ± 0.5 °C and the heating and cooling rates were measured with a precision of 10% or better. The temperature was controlled by a microprocessor.

III. RESULTS

A. Piezoelectric response

The piezoelectric strain was measured with the Mach–Zehnder interferometer (Fig. 1) with a small ac drive voltage

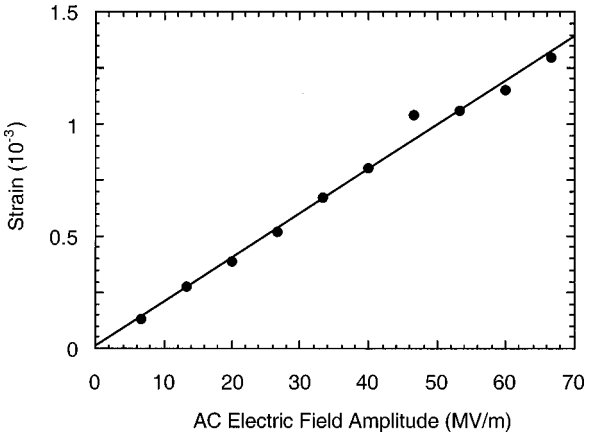

FIG. 2. Plot of piezoelectric strain vs amplitude of the 1 kHz ac electric field applied across the film.

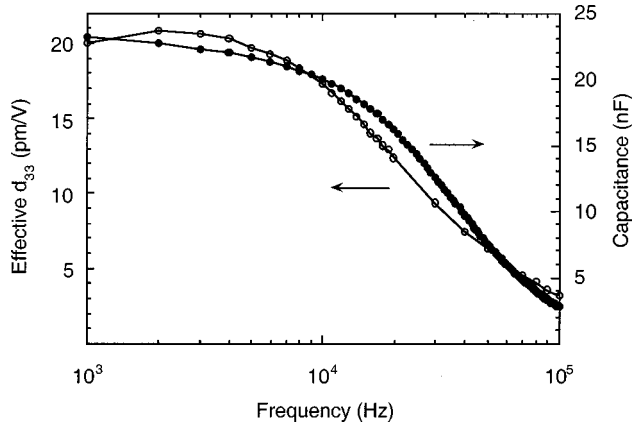

FIG. 3. Plot of effective piezoelectric coefficient d_{33}(eff) and capacitance vs frequency f of the ac electric field. The magnitude of the field was 6.7 MV/m.

V_{ac} (too small to disturb the net polarization) at frequency $f=1$ kHz. The strain increased linearly with the amplitude of the ac field, as shown in Fig. 2, and the slope of this line was equal to the effective piezoelectric coefficient d_{33}(eff) $=-20\pm2$ pm/V. The negative sign of the piezoelectric coefficient was determined by considering the direction of the spontaneous polarization and the direction of changes of film thickness caused by the driving ac field. The effective piezoelectric coefficient gradually decreases with increasing frequency as does the capacitance in the frequency range 1–100 kHz, as shown in Fig. 3.

B. Pyroelectric response

The absolute value of the pyroelectric coefficient of the 30 ML film was measured using the slow heating/cooling method at zero dc voltage after the sample was polarized by a 24 V dc voltage. Figure 4 shows a typical temperature profile and the corresponding pyroelectric current. As the temperature increases, a negative current flows through the circuit, when the temperature decreases, the pyroelectric current is positive. Similar current patterns were also observed in control experiments with commercial polarized PVDF film. The pyroelectric current was proportional to the rate of temperature change, as shown in Fig. 5. The effective pyroelectric coefficient calculated from the data in Fig. 5 using Eq. (5) was $p_3(\text{eff})=-20\pm4\,\mu\text{C/m}^2\,\text{K}$ at temperature 20 °C. The temperature dependence was measured by the Chynoweth modulation method and is presented in Fig. 6. There is a maximum of the pyroelectric current at a temperature of 88 °C while heating, corresponding to the ferroelectric–paraelectric phase transition.[8] The 30 ML films retain their pyroelectric and piezoelectric properties for at least several months if kept at room temperature.

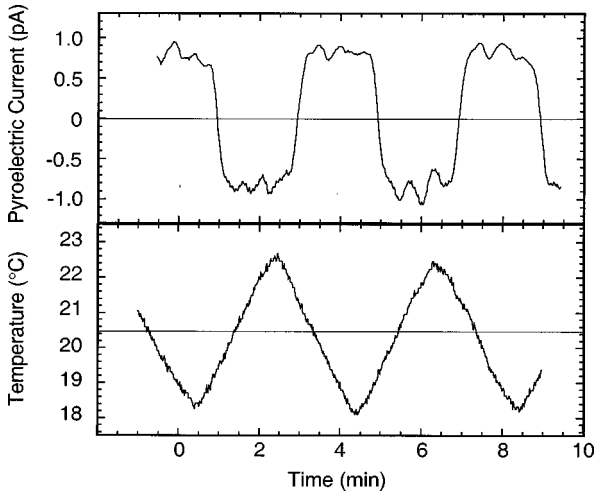

FIG. 4. Temperature cycle for the slow heating/cooling method applied to the sample and the resulting pyroelectric current response cycled around 20 °C.

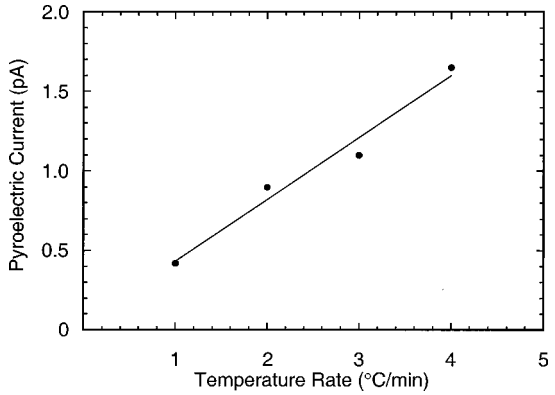

FIG. 5. Plot of pyroelectric current vs rate of temperature change at temperature 20 °C for the slow heating/cooling method.

C. Switching

Figure 7 shows the effect of ferroelectric polarization direction reversal (switching) on both piezoelectric and pyroelectric responses with the same sample. A dc voltage initially set to −16 V (applied to the top electrode) was increased step by step to +16 V, then returned to −16 V. For each step, we maintained the voltage constant for 10 min and removed the dc voltage during brief measurements. (This latter precaution eliminates contributions to the strain from electroattraction and electrostriction.) We measured the piezoelectric coefficient and the pyroelectric current (using the

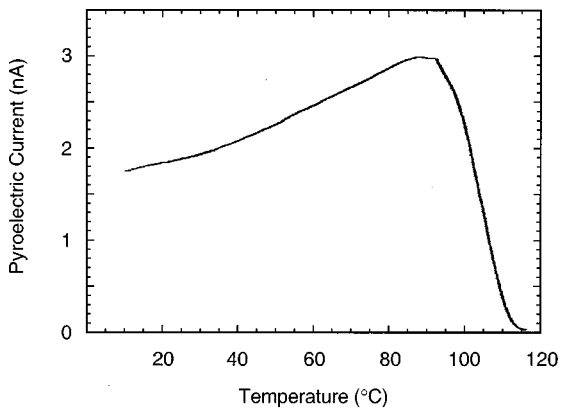

FIG. 6. Plot of the pyroelectric current measured by the Chynoweth method vs temperature.

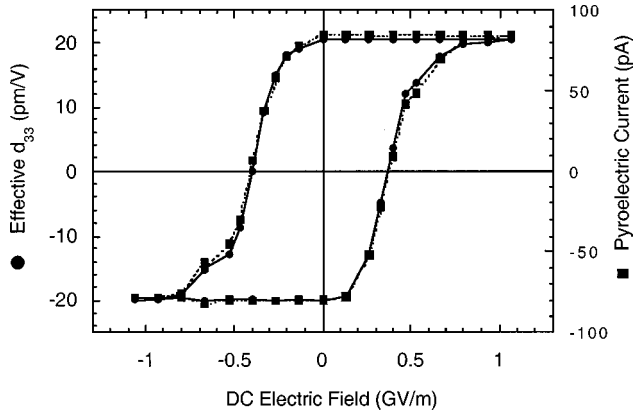

FIG. 7. Hysteresis of the effective piezoelectric coefficient d_{33}(eff) and the pyroelectric current as the applied dc electric field was cycled at room temperature.

Chynoweth method[6]) with the same laser beam, on the same sample area, and with the same polarization state, also at zero dc bias. The nearly rectangular shape of the hysteresis (Fig. 7) indicates a high degree of crystallinity and uniformity. The coercive fields in both piezoelectric and pyroelectric measurements show an excellent match at 4×10^8 V/m, comparable to other ultrathin P(VDF/TrFE) films,[6–9] and ten times larger than the coercive field in the typical thick films made by solvent spinning.[18] The piezoelectric coefficient is proportional to the pyroelectric current in all polarization states (at each point in Fig. 4) because both are proportional to the spontaneous polarization.[17] This is shown in Fig. 8 with the values taken from the data in Fig. 7.

IV. DISCUSSION

We demonstrated the piezoelectric and pyroelectric response in ultrathin copolymer P(VDF/TrFE) films (thickness about 15 nm) and measured the absolute values of the piezocoefficient d_{33}(eff) and pyrocoefficient p_3(eff) at room temperature, which are summarized in Table 1. The piezoelectric (-20 pm/V) and pyroelectric (-20 μC/m^2 K) coefficients are only slightly lower than those measured in spun films [-40 pm/V (Ref. 5) and -35 μC/m^2 K (Ref. 19)], verifying again[7–9] that these ultrathin films have essentially the same

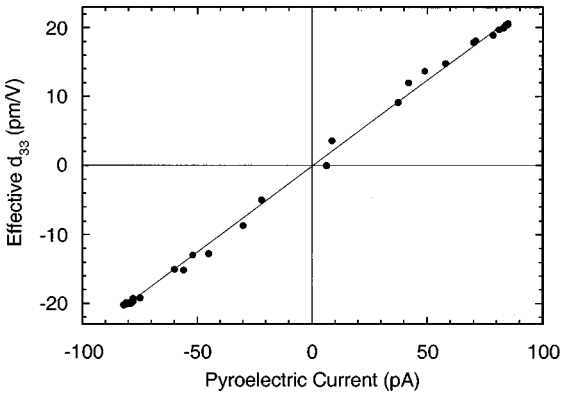

FIG. 8. Plot of effective piezoelectric coefficient d_{33}(eff) vs pyroelectric current for all polarizing states (data from Fig. 7).

TABLE I. Comparison of the piezoelectric and the pyroelectric coefficients of LB films and spun films.

Material	d_{33}(eff) (pm/V)	p_3(eff) (μC/m^2 K)	P_s (C/m^2)
LB film	-20 ± 2	-20 ± 4	0.1[d]
Spun film	-40[a]	-35[b]	0.1[c]

[a]Reference 5.
[b]Reference 19.
[c]Reference 18.
[d]Reference 7.

bulk ferroelectric behavior as much thicker spun films. The fully stress-free piezoelectric coefficient d_{33}^T can be as much as 70% higher then the measured d_{33}(eff), as we estimated by Eq. (2) in the case of PVDF for which all the needed elastic compliance constants are available.[20] The piezoelectric properties in ferroelectric materials arise from the electrostriction coupling with spontaneous polarization P_s as follows:[15,17]

$$d_{33}=2\epsilon_{33}\epsilon_0 k_{33}P_s, \tag{6}$$

where ϵ_{33} is dielectric constant, ϵ_0 is vacuum dielectric constant, and k_{33} is the (quadratic) electrostriction coefficient. Calculations by Eq. (6), where $\epsilon_{33}=8$,[8] $k_{33}=-2.3\,\mathrm{m}^4/\mathrm{C}^2$,[5] and $P_s=0.1\,\mathrm{C/m}^2$,[7] gives $d_{33}=-32$ pm/V, in reasonable agreement with experimental results (-20 pm/V). Equation (6) also explains why the piezoelectric coefficient has approximately the same frequency response as the dielectric constant (or the capacitance), as shown in Fig. 3. This result and the proportionality of d_{33} to p_3 demonstrated in Fig. 8 support the electrostriction coupling model as a basic mechanism of the piezoelectric effect in ferroelectric polymers.[5] By using the temperature dependence of the pyroelectric current (Fig. 6) and the value of spontaneous polarization at room temperature,[7] we calculated the expected value of the primary pyroelectric coefficient at room temperature $p_3=dP_s/dT=-830\,\mu\mathrm{C/m}^2\,\mathrm{K}$. The phenomenological Devonshire theory[17] predicts

$$p_3=-\epsilon_{33}\beta P_s, \tag{7}$$

where $\epsilon_{33}=8$ (Ref. 8) is the dielectric constant; $\beta=6.7\times10^{-4}\,\mathrm{K}^{-1}$ is the inverse Curie constant, calculated from the temperature dependence of the dielectric constant (Fig. 2 of Ref. 8, $\epsilon_\infty=4$); and P_s is the spontaneous polarization [0.1 C/m^2 (Ref. 6)]. From Eq. (7), we calculate $p=-530\,\mu\mathrm{C/m}^2\,\mathrm{K}$ at room temperature. Both of these calculated values are much higher than 20 μC/m^2 K, as was measured directly (from Fig. 4). This discrepancy has also appeared in studies of the thicker spun films, where the observed pyroelectric coefficient of -35 μC/m^2 K (Ref. 19) is much smaller than the expected value of $dP_s/dT=-220\,\mu\mathrm{C/m}^2\,\mathrm{K}$ (taken from Fig. 3 of Ref. 18) and the value $p=-310\,\mu\mathrm{C/m}^2\,\mathrm{K}$, calculated from Eq. (7), with $\epsilon_{33}=10$, $\beta=3.1\times10^{-4}\,\mathrm{K}^{-1}$, and $P_s=0.1\,\mathrm{C/m}^2$, all data from Ref. 18. This discrepancy can be explained, at least partially, by the strong secondary pyroelectric effect contribution given by the second term in Eq. (5). We calculated the secondary pyroelectric effect contribution in the range -40 to

$-580\ \mu C/m^2\,K$, for different sources of elastic compliance coefficient s_{33} and piezoelectric coefficient d_{33} for spun P(VDF/TrFE) films.[19,21,22] Disappearance of the pyroelectric response at temperatures above the phase transition point (Fig. 6), and hysteresis behavior of the pyroelectric and piezoelectric responses, show the true ferroelectric nature of the pyroelectric and piezoelectric effects in LB copolymer P(VDF/TrFE) films. One of the advantages of LB ferroelectric films compared with traditional spun films is the low polarizing and driving voltages (Fig. 7 and 2). We hope these types of LB films with significant piezoelectric and pyroelectric response will find their place in molecular electronics and as a material for sensors.

ACKNOWLEDGMENTS

This work was supported by the National Science Foundation and by the Nebraska Research Initiative through the Center for Materials Research and Analysis. Work at the Institute of Crystallography was supported by INTAS Project No. 93-1700.

[1] H. Kawai, Jpn. J. Appl. Phys. **8**, 975 (1969).
[2] J. G. Bergman, Jr., J. H. McFee, and G. R. Crane, Appl. Phys. Lett. **18**, 203 (1971).
[3] E. Fukada, Phase Transit. **18**, 135 (1989).
[4] K. Tashiro, M. Kobayashi, H. Tadokoro, and E. Fukada, Macromolecules **13**, 691 (1980).
[5] T. Furukawa and N. Seo, Jpn. J. Appl. Phys., Part 1 **24**, 675 (1990).
[6] A. Bune, S. Ducharme, V. Fridkin, L. Blinov, S. Palto, N. Petukhova, and S. Yudin, Appl. Phys. Lett. **67**, 3975 (1995).
[7] S. Palto, L. Blinov, E. Dubovik, V. Fridkin, N. Petukhova, A. Sorokin, K. Verkhovskya, S. Yudin, and A. Zlatkin, Europhys. Lett. **34**, 465 (1996).
[8] A. V. Bune, V. M. Fridkin, S. Ducharme, L. M. Blinov, S. P. Palto, A. V. Sorokin, S. G. Yudin, and A. Zlatkin, Nature (London) **391**, 874 (1998).
[9] S. Ducharme, A. V. Bune, L. M. Blinov, V. M. Fridkin, S. P. Palto, A. V. Sorokin, and S. G. Yudin, Phys. Rev. B **57**, 25 (1998).
[10] J. Choi, P. A. Dowben, A. Bune, M. Poulsen, S. Pebley, S. Adenwalla, S. Ducharme, W. A. Hamilton, V. M. Fridkin, S. P. Palto, N. Petukhova, and S. G. Yudin (unpublished).
[11] S. Ducharme, J. Feinberg, and R. R. Neurgaonkar, IEEE J. Quantum Electron. **QE-23**, 2116 (1987).
[12] J. F. Nye, *Physical Properties of Crystals* (Clarendon, Oxford, 1979).
[13] K. Lefki and G. J. M. Dormans, J. Appl. Phys. **76**, 1764 (1994).
[14] J. F. Legrand, Ferroelectrics **91**, 303 (1989).
[15] A. G. Chynoweth, J. Appl. Phys. **27**, 78 (1956).
[16] G. G. Roberts, Ferroelectrics **91**, 21 (1989).
[17] M. E. Lines and A. M. Glass, *Principles and Application of Ferroelectrics and Related Materials* (Clarendon, Oxford, 1977).
[18] T. Furukawa, Phase Transit. **18**, 143 (1989).
[19] R. Kohler, G. Gerlach, P. Padmini, G. Hofmann, and R. Bruchhaus, J. Korean Phys. Soc. **32**, s1744 (1998).
[20] Y. Xu, *Ferroelectric Materials and Their Applications* (North-Holland, Amsterdam, 1991).
[21] J. K. Kruger *et al.*, Phys. Rev. B **55**, 3497 (1997).
[22] J. Petzelt, J. F. Legrand, S. Pacesova, S. Kamba, G. V. Kozlov, and A. A. Volkov, Phase Transit. **12**, 305 (1988).